JOURNAL OF MATERIALS SCIENCE 29 (1994) 4357–4370

A kinetic and morphological study of the coking of some heat-resistant steels

D. R. G. MITCHELL, D. J. YOUNG
School of Materials Science and Engineering, University of New South Wales, P.O. Box 1, Kensington, New South Wales, 2033, Australia

The coking behaviour of a range of austenitic, heat-resistant steels has been examined in the temperature range 700–1000 °C. At and below 800 °C, catalytic coke in the form of bundles of filaments formed at localized defect sites in the carbide scales. A wide range in weight-gain kinetics resulted from the differing efficacy of the non-catalytic carbide scales in excluding carbon from the catalytically active substrate. At and above 900 °C, catalytic coke formation gave way to pyrolytic coke formation and internal carburization became significant. Parabolic kinetics resulted from the fact that internal carburization was rate-determining. Carburizing alloys gained weight an order of magnitude faster than did alloys protected by oxide films. This was a consequence of dissolution of carbon into the alloy directly from the gas stream being much faster than the rate of coke formation on the alloy surface. Oxide-protected alloys all gained weight at a similar rate, the rate being that of coke deposition on coke. Oxide films containing aluminium were more effective in excluding carbon from the alloy than chromium-containing oxides. However, under reducing conditions, preformed oxide films were not beneficial in limiting carburization in the longer term, because they were prone to spalling, cracking and conversion to non-protective carbide.

1. Introduction

Steam cracking is an important industrial process for the conversion of hydrocarbon fractions into olefins. This involves the cracking of hydrocarbon gases in the presence of steam, by passing the gas mixture through pyrolysis tubes, radiantly heated to temperatures as high as 1100 °C [1, 2]. The corrosive nature of this environment, the high temperature and the mechanical stresses experienced by the pyrolysis furnace tubes, dictate the use of high-performance alloys in their construction. In recent years, the choice of materials for such applications has been HP grade cast austenitic heat-resistant steel. These alloys typically contain 25 wt % chromium to impart good corrosion resistance, and 35 wt % nickel to give high strength and creep resistance, and are often niobium-stabilized. Despite their excellent high-temperature behaviour in oxidizing environments, such alloys experience carburization attack when exposed to carbon-containing gas streams. Carbon can dissolve in the alloy leading to the formation of internal carbide precipitates. This can cause degradation of the chemical and mechanical properties of the alloy, leading to premature tube failure [2–4]. As a result of its industrial significance, the phenomenon of internal carburization has been widely studied [1–16] and the mechanism is now fairly well understood.

Apart from contributing to carburization, the bulky coke which forms on the tube surface is undesirable in several other respects. It represents a loss of product, it restricts the tube bore causing pressure drops, and it impairs heat flow leading to reduced process efficiency [17–19]. In addition, localized overheating of the furnace tubes may occur. The rates of coke formation on several alloy systems important to steam cracking applications have been studied [19–21]. The kinetics of coke formation on an alloy surface are governed by a wide range of factors, an important one of which is the catalytic activity of the alloy, which is itself a function of the alloy composition [20]. For example, nickel and nickel-rich alloys are known to catalyse coke deposition, and are widely used industrially as catalysts for hydrocarbon conversion [22], while copper shows no catalytic activity [20]. In industrial practice, the problem of coke build-up in pyrolysis furnaces is countered by periodically decoking furnace tubes by passing through steam at high temperature to gasify the coke. This results in expensive process down-time, and induces cyclic thermal stresses on the tube assemblies.

The development of alloys which not only resist carburization attack, but are also non-catalytic towards coke deposition, is highly desirable. The present work is concerned with evaluating the coking behaviour of some novel heat-resistant alloys, some of which contain reactive element additions. As part of this study, the carburization behaviour of these alloys in purely carburizing (reducing) conditions [23] and steam carburizing (mildly oxidizing) conditions [24] have also been assessed.

0022–2461

2. Experimental procedure

The kinetics of coke deposition from a hydrogen–propylene atmosphere were monitored continuously using a C. I. Electronics MK IIB Microforce microbalance. The experimental arrangement has been described elsewhere [20]. Specimens were held in a silica cradle, and suspended on a silica thread inside a Vycor tubular reactor. The reactor was heated externally by an electric furnace, and temperature was controllable to $\pm 2\,^{\circ}C$. The specimen temperature was monitored by an external thermocouple alongside the tubular reactor. High-purity hydrogen and propylene were passed through calibrated flow meters to the reactor, with a hydrogen:propylene volume ratio of 89:11. A continuous purge of 35 ml min^{-1} hydrogen was passed through the microbalance head to shield it from the corrosive atmosphere, and 500 ml min^{-1} hydrogen, and 66 ml min^{-1} propylene were passed directly into the reactor, giving a total flow rate 601 ml min^{-1}. Gas residence time in the reactor hot zone at 1000 °C was approximately 5 s.

Eight austenitic alloys containing 18–24 wt % Cr and 32–39 wt % Ni were supplied by Schmidt and Clemens GmbH for testing. The alloys contained various minor reactive element additions as shown in Table I. Alloy A was a commercially available HP grade steel, designated G 4852 (MOD A), while the remaining alloys were experimental grades. Alloys A, B and C were supplied in the form of rods approximately 9.5 mm diameter, cut from centricast tubes, while alloys D–H were investment castings, being rods of 10 mm diameter. Metallographic examination of the as-received alloys showed that they all contained primary interdendritic carbides. Specimens were cut in the form of discs using a diamond saw, and subsequently ground to a 600 grit finish. They were then ultrasonically degreased in acetone, and weighed. Specimen surface areas were approximately 2 cm^2.

Following purging of the system with argon for 45 min, a high flow rate of hydrogen was passed through for a minimum of 30 min. The pre-heated furnace was then raised over the reactor tube and the system allowed to attain thermal equilibrium. This took 15–30 min depending on the temperature. Propylene was then introduced, whereupon weight gain was observed to commence. Cracking of the hydrocarbon to produce polycyclic tars and coke occurred, though no analysis of the reaction products was undertaken. Specimens were reacted at 700, 800, 900 and 1000 °C for durations of up to 300 min. The largest total weight gains recorded were approximately 2.5 mg cm^{-2}. At the end of each test, the furnace was lowered, and the specimen allowed to cool in the flowing gas. After every test, the reactor tube, cradle and thread were decoked, by passing air through the system at 800 °C. This ensured the same surface conditions inside the reactor at the start of every test. Weight changes of the thread and cradle on decoking were measured, and these were usually insignificant in comparison to the weight change of the alloys. Specimens were examined using optical microscopy and scanning electron microscopy (SEM) with energy dispersive analysis of X-rays (EDX) facilities. Transmission electron microscopy (TEM) and X-ray diffraction (XRD) were also used.

3. Results

3.1. Kinetics

At 700 °C, only four alloys were tested (Fig. 1). Weight gains were very small, being not much greater than the sensitivity of the balance ($\pm$ 0.02 mg), and consequently the scatter in the results was quite large. However, the kinetics appeared to be linear. At 800 °C (Fig. 2) the kinetics were also linear, usually after an initial period of fairly rapid weight gain. Only alloy E exhibited parabolic kinetics at this temperature. The slopes

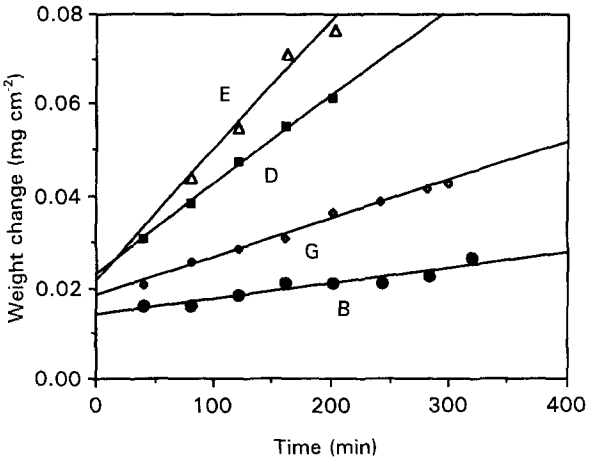

Figure 1 Weight-gain kinetics for alloys exposed to flowing hydrogen–propylene atmosphere at 700 °C.

TABLE I Chemical composition of alloys (wt %) (Fe balance)

Alloy	C	Si	Mn	Cr	Mo	Ni	Zr	Nb	Ti	Ta	Hf
A	0.45	1.8	1.1	24.0		32.3	0.1	0.8	0.2		
B	0.4	2.6	1.0	24.0		32.4	0.05	0.8	0.1		
C	0.4	1.8	1.2	24.0	3.1	32.2	0.1	0.7	0.3		
D	0.4	1.45	0.4	22.3	3.3	37.4	0.5	0.4	0.4	0.7	1.3
E	0.4	1.8	0.4	23.1	3.5	39.1	0.2	0.4	0.3	0.8	0.9
F[a]	0.45	1.35	0.4	23.3	3.1	31.2	0.2	0.3	0.2	0.8	0.6
G	0.4	2.0	0.35	18.8	3.1	33.0	0.4	0.4	0.2	1.2	0.9
H[b]	0.4	0.7	0.4	17.7	3.1	31.3	0.5	0.4	0.3	1.2	1.3

[a] Contains 14.8 wt % Co.
[b] Contains 1.65 wt % and 14.3 wt % Co.

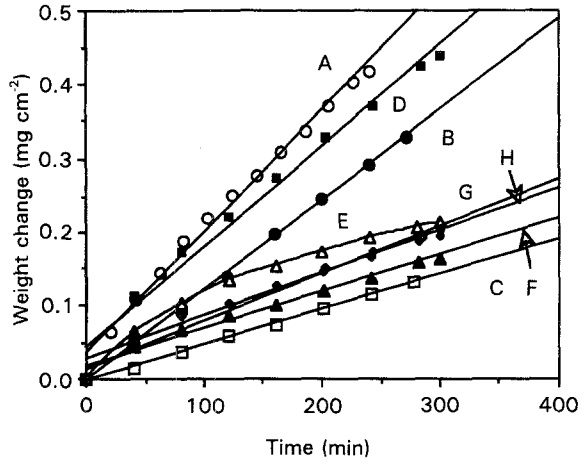

Figure 2 Weight-gain kinetics for alloys exposed to flowing hydrogen–propylene atmosphere at 800 °C.

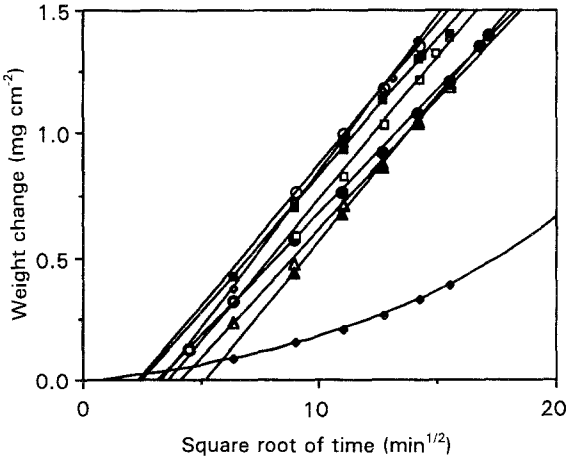

Figure 3 Weight-gain kinetics for alloys exposed to flowing hydrogen–propylene atmosphere at 900 °C. (○) A, (●) B, (□) C, (■) D, (△) E, (▲) F, (◇) G, (◆) H.

of the linear portion of the weight gain per unit area versus time plots at 700 and 800 °C, yielded linear rate constants, k_{lin}, which are shown in Table II. Substantial differences exist among the alloys.

At 900 °C (Fig. 3), all the alloys exhibited parabolic behaviour except alloy H, which showed linear weight-gain kinetics at this temperature. At 1000 °C, all alloys displayed parabolic behaviour (Fig. 4), although alloy H produced weight-gain kinetics which ranged between these two regimes (Fig. 5). It was also distinctive at the two higher temperatures in that it displayed weight-gain rates much less than the other alloys. Plots of weight gain versus square root of time yielded straight lines at 900 and 1000 °C (Figs 3 and 4). Although it is difficult to identify individual alloy kinetics in these figures, the important point demonstrated is the similarity of the kinetic behaviour of all the alloys except H. The kinetics could be described by the parabolic equation

$$\frac{\Delta W}{A} + W' = (2k_p t)^{1/2} \quad (1)$$

where $\Delta W/A$ is the weight change per unit area, W' and k_p are constants and t is time. Linear regression of the data on the above equation enabled these constants to be estimated (Table II). In general, the straight line fits were better at the higher temperature. At 1000 °C, the rate constant for alloy H was more than an order of magnitude smaller than that for alloy G, which had the highest k_p values for the alloy set.

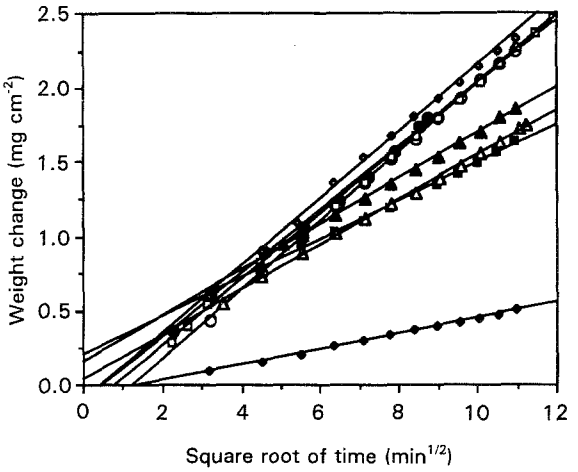

Figure 4 Weight-gain kinetics for alloys exposed to flowing hydrogen–propylene atmosphere at 1000 °C. For key, see Fig. 3.

TABLE II Linear rate constants, k_{lin}, at 700 and 800 °C and parabolic rate constants, k_p, and activation energies, E, at 900 and 1000 °C for alloys reacted in a flowing hydrogen–propylene atmosphere

Alloy	k_{lin} (10^{-3} mg cm^{-2} min^{-1})		k_p (10^{-3} mg^2 cm^{-4} min^{-1})		E (kJ mol^{-1})
	700 °C	800 °C	900 °C	1000 °C	
A		1.5	5.5	22.25	175
B	0.035	1.3	3.6	21.0	220
C		0.5	5.0	22.0	185
D	0.19	1.2	4.65	10.0	95
E	0.35	0.08[a]	3.65	12.0	145
F		0.45	3.95	13.5	150
G	0.08	0.6	5.5	23.5	180
H		0.5	1.5[b]	1.1[a]	–
				4.3[b]	

[a] $k_p \times 10^{-3}$ mg^2 cm^{-4} min^{-1}.
[b] $k_{lin} \times 10^{-3}$ mg cm^{-2} min^{-1}.

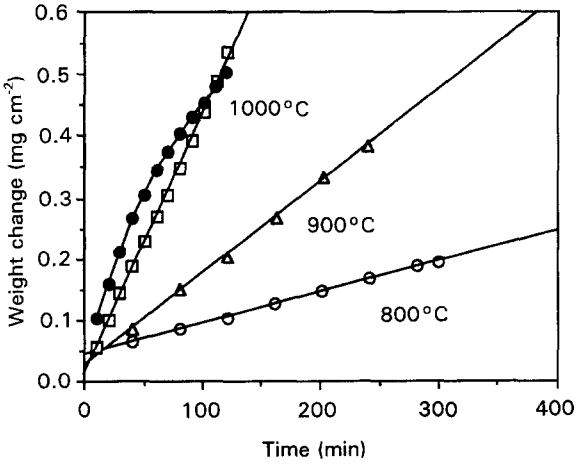

Figure 5 Weight-gain kinetics for alloy H at various temperatures, showing variable behaviour at 1000 °C.

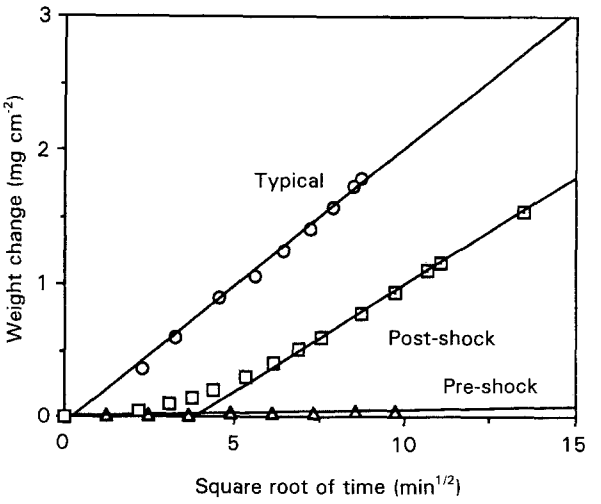

Figure 6 The effect of an oxide film on alloy B (formed during heat up) on the weight-gain kinetics at 1000 °C (pre-shock-plotted versus time rather than time$^{1/2}$). The kinetics after thermally shocking this film are shown also (post-shock).

The order of the alloys in terms of decreasing k_p values was very similar at the two highest temperatures.

Activation energies for the diffusion-controlled reaction occurring at and above 900 °C were determined from Arrhenius plots. The activation energies (Table II) were found to lie in the range 145–220 kJ mol^{-1}, while the result for alloy D was very low (95 kJ mol^{-1}). These values must be treated with caution as they are derived from only two data points.

In a few instances, deviation from the normal coking behaviour was observed at 1000 °C. This involved alloys displaying very low linear rates of weight gain, whereas high parabolic rates were measured usually. This was believed to result from the formation of a semi-protective oxide film on the specimen surface during heating-up in hydrogen at the start of the test, because it tended to occur only when gas purging prior to testing was carried out for a short period. This presumably left a relatively high residual concentration of oxidizing impurities in the reactor. It was also more prevalent following tests in which steam had been introduced into the reactor during decoking operations. An example of this "passivation" phenomenon is shown in Fig. 6. In the test in which passivation occurred (labelled Pre-shock), a very low linear rate of 4.2×10^{-3} mg cm^{-2} min^{-1} was observed.

The effect of a thermal shock on this behaviour was investigated by lowering the furnace and allowing the reaction tube to cool rapidly to room temperature. Hydrogen was passed through the reactor while cooling occurred. The furnace was then raised, and once thermal equilibrium had been attained, propylene was re-introduced and the post-shock coking rate determined. The post-shock coking rate was found to increase with time, until after about 60 min a parabolic rate was established. The post-shock parabolic rate (8.5×10^{-3} mg^2 cm^{-4} min^{-1}) was close to the normal parabolic rate for this alloy.

To establish if pre-oxidation did result in "passivation", alloy A was oxidized in dry air at 900 °C for 200 min. Previous results [25] have shown that this treatment leads to the development of a mixed scale of

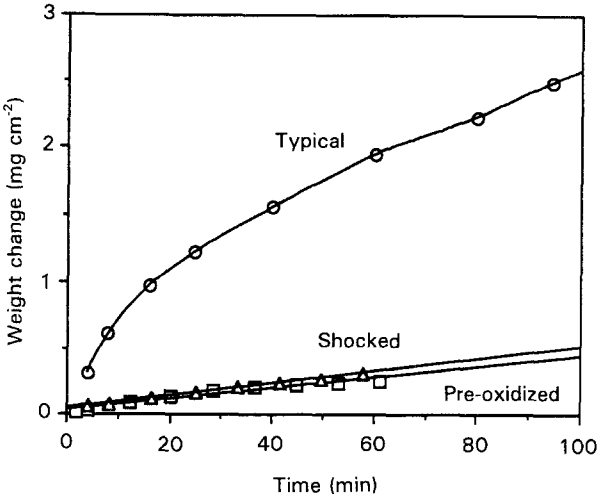

Figure 7 The effect of an oxide film, formed by pre-oxidation, on the weight-gain kinetics of alloy A at 1000 °C (pre-oxidized). The kinetics after thermally shocking this film are shown also (shocked).

Cr_2O_3 and $(Fe,Cr)_3O_4$. It can be seen (Fig. 7) that the presence of a pre-formed oxide scale did indeed modify the kinetics in a manner similar to that observed during passivation. A low linear rate was established following a slightly more rapid weight gain during the first 30 min. The linear rate constant was 2.2×10^{-3} mg cm^{-2} min^{-1}. The effect of a thermal shock on the coking rate of the pre-oxidized specimen was examined by lowering then raising the furnace in a manner identical to that just described. The post-shock coking rate increased only slightly, and remained linear, with a rate constant of 4.6×10^{-3} mg cm^{-2} min^{-1}.

Previous studies on these alloys at high temperature have shown that internal carburization was extensive at 900 °C and higher [16]. It was apparent, therefore, that the weight gain measured in these experiments consisted of two components: one due to coke deposition on the alloy surface, and a second due to internal

carburization. The former could be determined readily, by decoking coked specimens. The rate of coke build-up on the surface was determined for alloy A at 1000 °C only. The rate was determined by coking for various periods, then lowering the furnace to freeze the reaction and prevent further coke dissolution into the alloy. The furnace was cooled to 750 °C, during which time the reactor tube was purged with argon. Once at temperature, the furnace was raised and the system was allowed to reach thermal equilibrium. Measurements of the rate of internal carburization of this alloy (Table III) suggested that the rate of coke dissolution into the alloy would be insignificant at this temperature during the course of the experiment. Dry air was then passed into the reactor to burn off the coke, and a weight loss was recorded. Data accumulated in this way showed that the amount of coke on the alloy surface (Fig. 8) increased linearly with time ($k_{lin} = 1.1 \times 10^{-3}$ mg cm^{-2} min^{-1}) up to about 150–200 min. After this, the amount of carbon on the specimen surface increased more rapidly ($k_{lin} = 4.2 \times 10^{-3}$ mg cm^{-2} min^{-1}). The overall weight-gain kinetics were found to change from parabolic to linear around this time (Fig. 9) with the linear rate constant being 1.1×10^{-2} mg cm^{-2} min^{-1}.

TABLE III Alloy carburization depths after exposure to a hydrogen–propylene atmosphere at various temperatures

Alloy	Carburization depth (μm)			
	700 °C (5 h)	800 °C (4 h)	900 °C (4 h)	1000 °C (2 h)
A		0	100	180
B	0	20	120	150
C		0	100	175
D	0	35	80	135
E	0	20	75	125
F		0	85	170
G	0	0	110	195
H		0	[a]	[a]

[a] Internal attack localized and slight.

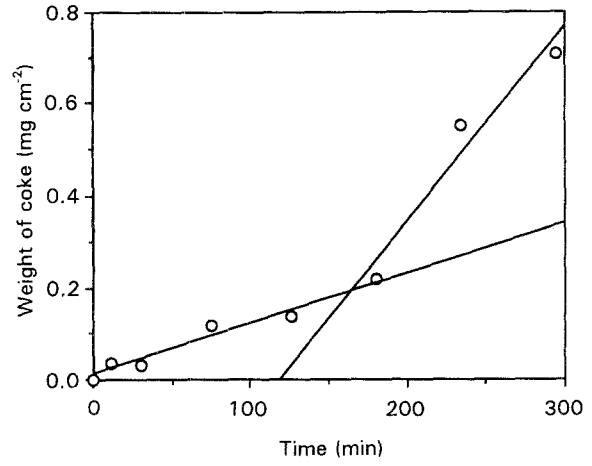

Figure 8 The rate of coke build-up on the surface of alloy A at 1000 °C, as measured by subsequent burn-off.

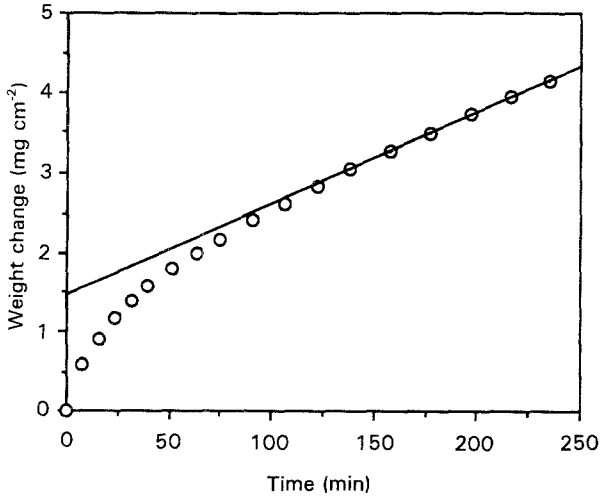

Figure 9 Weight-gain kinetics of alloy A after longer term coking at 1000 °C for 4 h. The kinetics change from parabolic to linear in longer tests.

3.2. Reaction morphologies

SEM, optical microscopy and XRD examination were carried out after testing, to investigate the morphological changes which occurred during coking. After exposure at 700 °C for 5 h, the only visual change was a slight tarnishing of the metallic lustre. The original surface grinding marks remained, and some small nodules developed (e.g. Fig. 10). These were found to be tight bundles of coke filaments with filament diameters of less than 1 μm. These were similar to nodules formed at 800 °C (Fig. 11). The surface compositions of all the alloys were found to be little changed after exposure, and stained cross-sections showed no internal carburization attack (Table III).

At 800 °C, a much greater change in the surface appearance took place. All alloys were discoloured by a thin layer of grey–black soot. Some larger blobs of soot (1–2 mm diameter) were occasionally visible, particularly on alloy A. SEM examination showed that many of the surfaces were covered with a fine-grained scale, and this was punctuated by an array of small surface nodules (Fig. 11). The nodules, the distribution of which replicated the dendritic structure of the alloy, were composed of bundles of tightly packed, fine coke filaments. Alloy B was the only alloy which did not have significant numbers of such nodules, and exhibited a granular scale instead. There appeared to be a loose correlation between the density of coke nodules on the surface and the weight-gain kinetics (ignoring alloy B). In general, those alloys with a high density of coke nodules on the surface, e.g. alloy A, exhibited the highest rate of weight gain, while those with a low or moderate density of low-volume nodules, e.g. alloy C, experienced the lowest rates.

XRD analysis showed that M_7C_3 and $M_{23}C_6$ (where M was predominantly chromium) were present on all alloys except H, which appeared to be unaffected. $M_{23}C_6$ was originally present in the alloys as an interdendritic phase, unlike M_7C_3, which was a reaction product. M_3C_2 was only detected, albeit tentatively, on alloy F at the highest temperature. Stained cross-sections showed that only alloys B, D

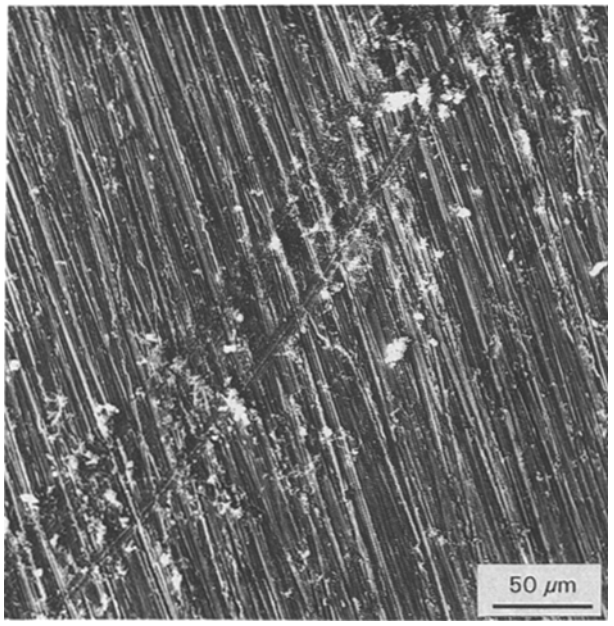

Figure 10 Scanning electron micrograph of the surface of alloy B after coking for 5 h at 700 °C, showing very limited coke formation.

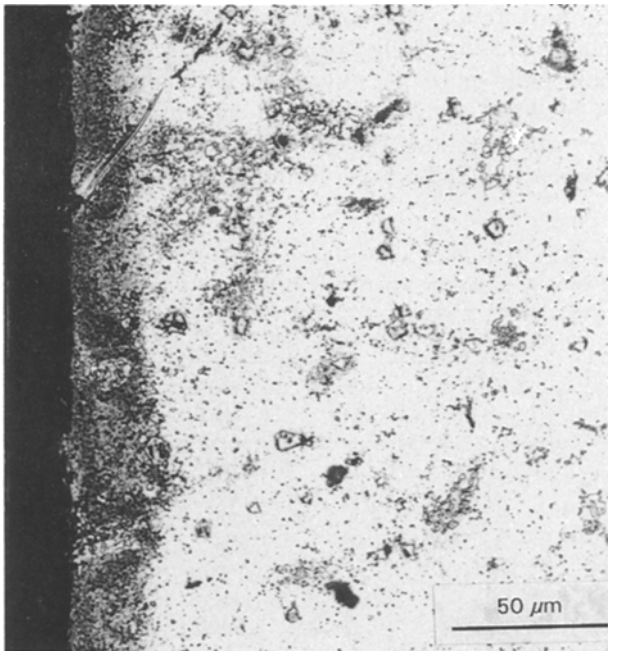

Figure 12 Optical micrograph of a cross-section of alloy D after coking for 4 h at 800 °C, stained to show relatively slight internal carburization.

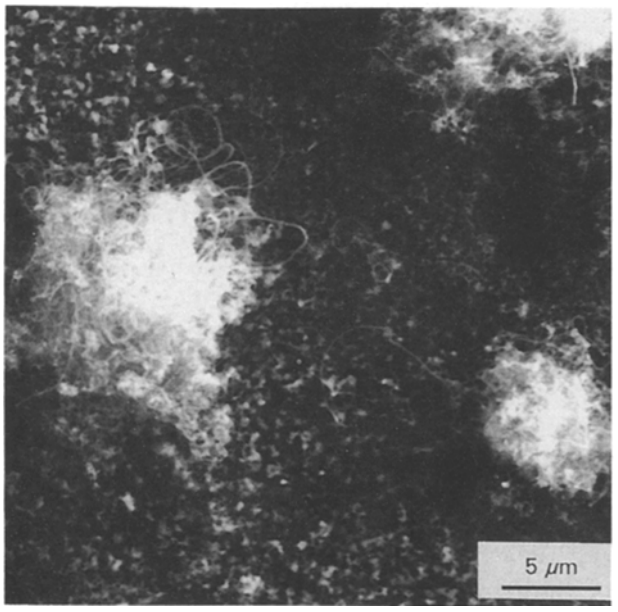

Figure 11 Scanning electron micrograph of the surface of alloy F after coking for 4 h at 800 °C, showing surface nodules consisting of bundles of thin coke filaments, growing through a granular surface carbide layer.

and E underwent slight internal attack (Table III). A typical example of this is shown in Fig. 12. Some external carbide scale formation was observed on alloys A–D. This scale was poorly adhered and appeared to spall readily. Very little internal attack and no external scale was evident on alloys F and G. Under these conditions, alloy H was the only alloy which neither underwent internal attack nor formed an external scale.

EDX analysis of the alloy surfaces showed that, in general, chromium, silicon (and aluminium in the case of alloy H), were enriched at the surface, compared with the original bulk compositions at all temperatures above 800 °C. In general, minor reactive elements (excluding silicon) were not found to segregate to the surface.

Alloy H was the only alloy to contain a significant amount of aluminium, and the surface concentration after exposure was found to increase from 1.65 wt % to 5 ± 1 wt %. The coke on this surface was blocky and coarse with some fine filaments growing from it (Fig. 13a). Metal-rich particles were found within this scale (Fig. 13b). EDX analysis showed that these particles were not catalytic to coke formation, because they were not associated with dense coke filament growth, and rather than being rich in nickel, they contained large amounts of the reactive elements zirconium, hafnium and aluminium. The coking rate of this alloy was amongst the lowest for the alloy set. The particles may well be small fragments of near-surface carbides, disrupted by coke growth. Isolated internal carbides rich in these reactive elements have been identified in this alloy [25].

Two alloys (A and F) formed several large (1–2 mm diameter) sooty growths on the surface (Fig. 14). These were found to be complex tangles of coarse filaments. Those filaments making up the typical surface nodules were less than 1 μm diameter, while those making up the coarse growths were somewhat thicker. Back-scattered electron images of coke growths on the surface of all the alloys except A failed to locate any catalytic metal particles, while on alloy A only a few were located. Spot analysis of these showed them to be nickel-rich. TEM examination of the coke filaments formed on alloy A (Fig. 15) showed them to be amorphous, and in some instances to have metallic particles at the growing tip. Convergent-beam EDX analysis showed these particles to be nickel-rich. They

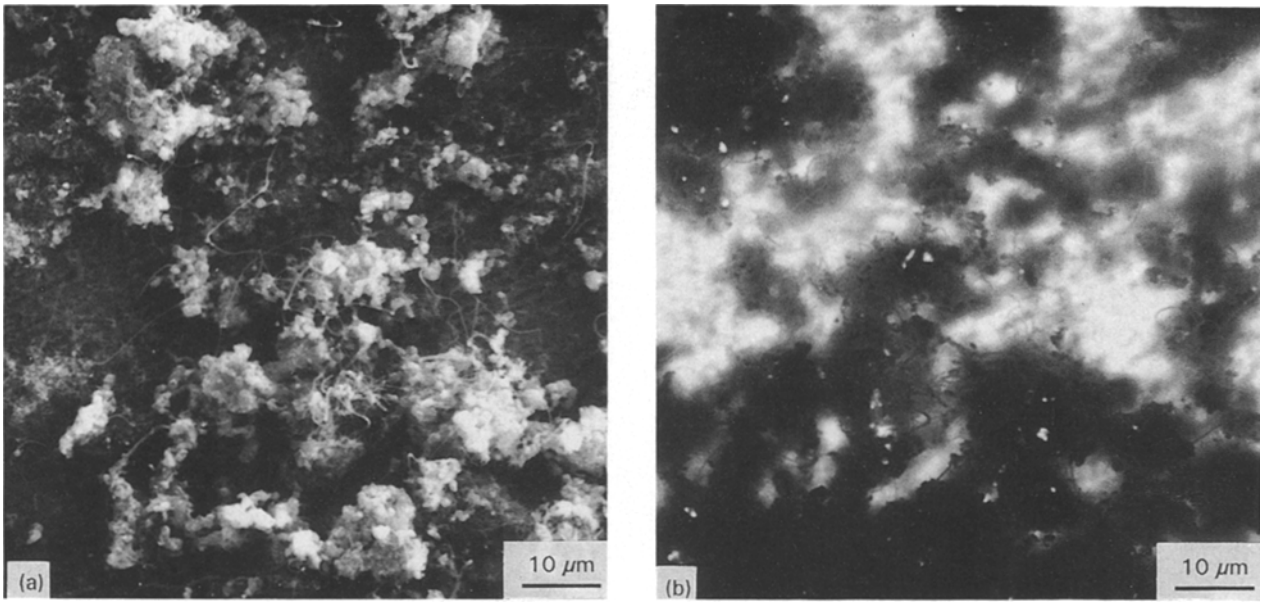

Figure 13 Scanning electron micrographs of the surface of alloy H after coking for 4 h at 800 °C, showing: (a) blocky and filamental coke; (b) backscattered electron image of (a) highlighting small fragments of reactive element-rich carbide (light) within the coke (dark).

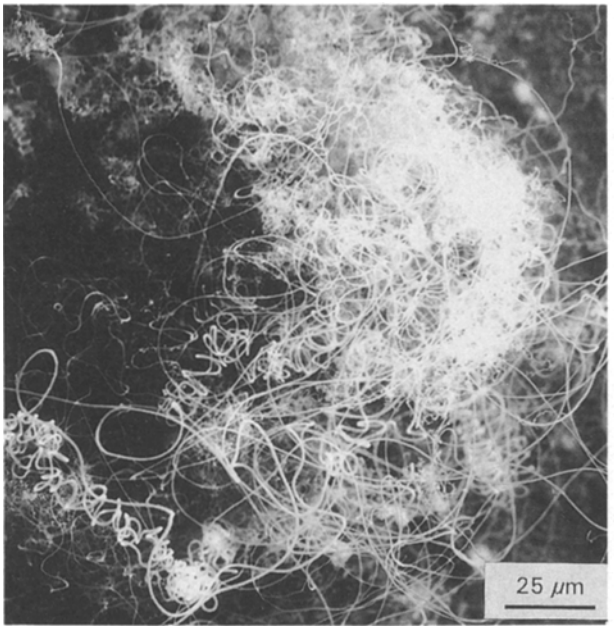

Figure 14 Scanning electron micrograph of a soot particle formed on alloy A after coking for 4 h at 800 °C, showing it to be a dense tangle of relatively coarse coke filaments.

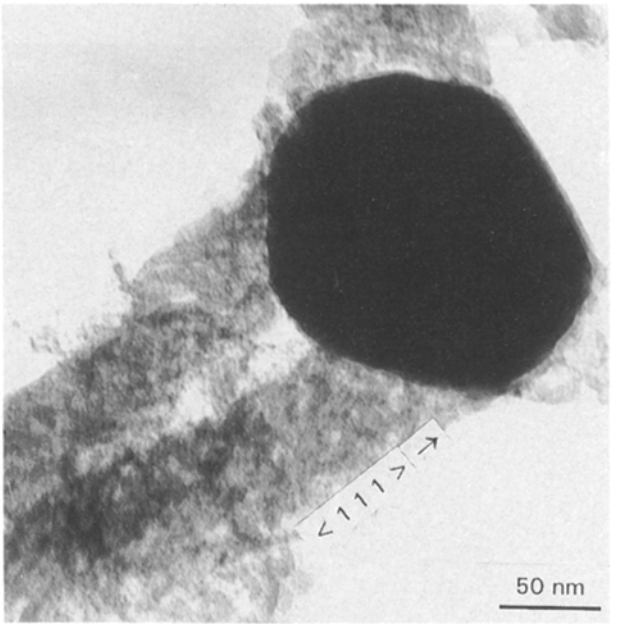

Figure 15 Bright-field TEM image of a nickel-rich particle found at the growing tip of a coke filament, formed on alloy A after coking for 4 h at 800 °C. The electron beam direction is ⟨1 1 2⟩, and the facet at the particle head is a Ni {1 1 1} plane.

were highly facetted and ranged in diameter between 100 and 500 nm. In every particle analysed by convergent-beam electron diffraction (CBED), the growth axis of the filament was always perpendicular to the {1 1 1} plane of the particle. This plane corresponded to the facet at the tip head. The smaller particles, which were sufficiently electron transparent to analyse using this technique, were found to be monocrystalline, with an f c c structure.

At 900 °C, all the alloys were covered with a matt black sooty film. SEM examination showed that the amount of surface coke was variable. The surface of alloy A had a granular surface layer of carbide (Fig. 16) with little or no filamental coke evident. Coke formation was evident on many of the other alloys at this temperature, and two types of coke were observed. These consisted of fine coke filaments along with some particulate coke, with a fluffy texture (e.g. Fig. 17). EDX analysis of the general surfaces of alloys A–G showed significant chromium enrichment, suggesting the surface be a chromium-rich carbide. Alloy H exhibited very low weight gains at this temperature, compared with the other alloys. It displayed significant surface enrichment of aluminium (11 wt %) along with slight enrichment of silicon and chromium. The reaction product was also very different from that

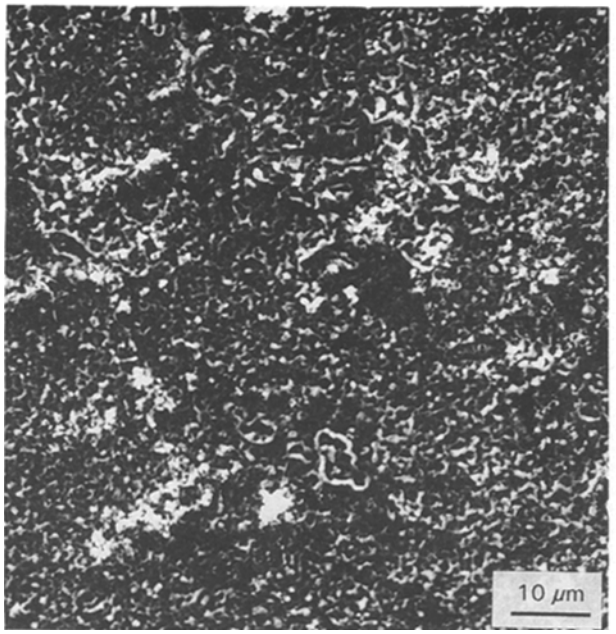

Figure 16 Scanning electron micrograph of the surface of alloy A after coking for 4 h at 900 °C, showing a granular carbide-covered surface with little coke evident.

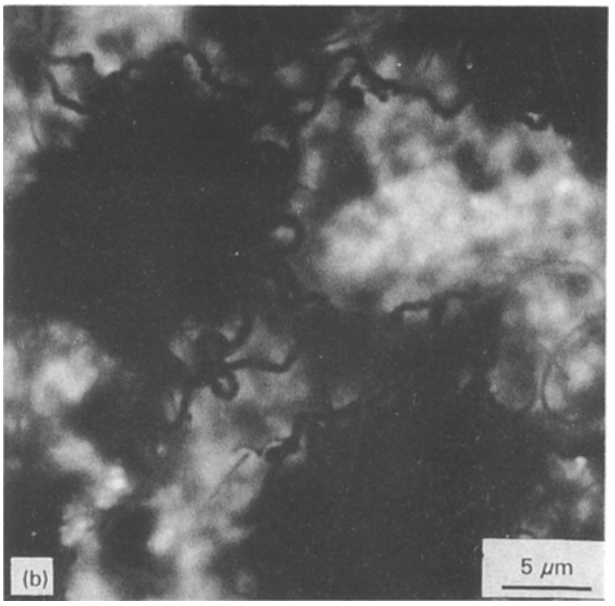

Figure 17 Scanning electron micrograph of the surface of alloy F after coking for 4 h at 900 °C, showing a dense surface layer of filamental and pyrolytic coke.

formed on the other alloys. The bulk of the surface appeared to be scattered with tangles of coarse coke filaments (Fig. 18a), which were much coarser than those seen on other alloys at 900 °C (e.g. Fig. 17), and devoid of metallic particles (Fig. 18b). There was little evidence for the formation of a granular surface scale of carbide, as original grinding marks were still present on the relatively smooth surface of the alloy (Fig. 18a, b). XRD analysis showed that all alloys formed M_7C_3 and coke except for H. This alloy formed coke, but no significant amounts of carbide.

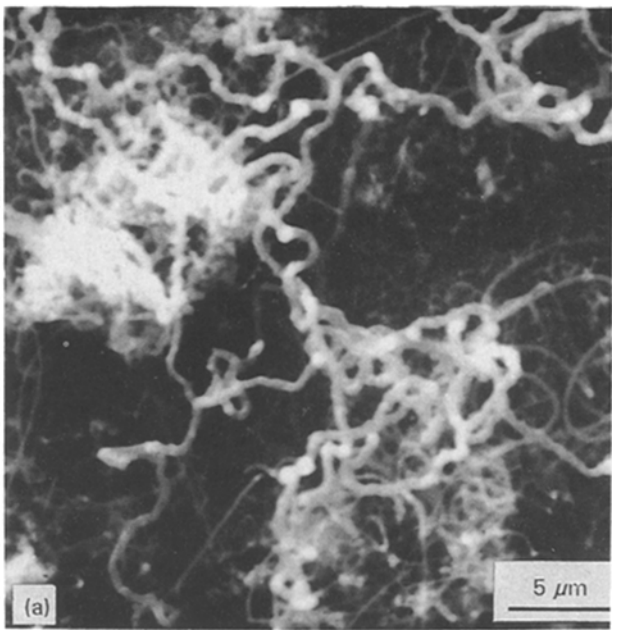

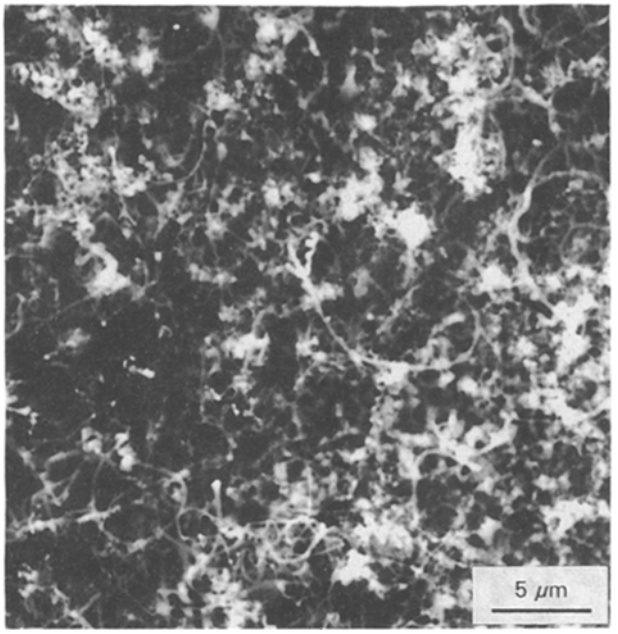

Figure 18 Scanning electron micrographs of the surface of alloy H after coking for 4 h at 900 °C, showing: (a) coarse filamental and nodular coke. The retained grinding marks and absence of granular carbide on the alloy show little or no carburization has occurred; (b) backscattered electron image of (a) distinguishing coke (dark) from unaffected alloy (light).

The diffraction peaks due to graphite were most intense on this alloy. Examination in section showed that only alloys A–C still had some carbide scale attached, although this was very poorly adhered. Internal attack was significant for all alloys except H (Table III). This alloy underwent very slight internal carburization, with the attack localized around dendrite boundaries.

All the alloys at 1000 °C formed a grey surface film, which varied from a matt grey to a bright metallic lustre. This was associated with carbide scale formation. Alloy H was the only alloy to form a sooty grey film at this temperature, which suggested the presence of coke. Alloys A–C displayed granular surfaces which imaged the dendritic structure of the underlying alloy

(e.g. Fig. 19). The surfaces of these alloys were enriched greatly in chromium. All the other alloys developed a smoother surface, scattered with small particles (Fig. 20). EDX analysis of these particles, suggested them to be pyrolytic coke rather than carbide. The general surface was not covered with a thick layer of coke, as total X-ray yields in EDX analysis were high, and what appeared to be fine-grained carbide could be seen projecting through this layer. Decoking experiments confirmed that little coke was present on the surface of alloy A: about 5% of the total weight gain observed during a 2 h test at 1000 °C was attributable to coke build up on the surface (cf. Figs 8 and 4). XRD analysis showed that all alloys except H formed M_7C_3, and M_3C_2 was detected on alloy F, which had the lowest iron content of the alloy set. There was too little coke to detect on all alloys except H, which exhibited an intense XRD peak due to coke. Stained cross-sections showed that all the alloys except H underwent severe internal attack at this temperature (Table III). Alloy G was the most severely carburized at this temperature (Fig. 21).

The nature of the attack on alloy H was unusual, with the attack being restricted to limited localized

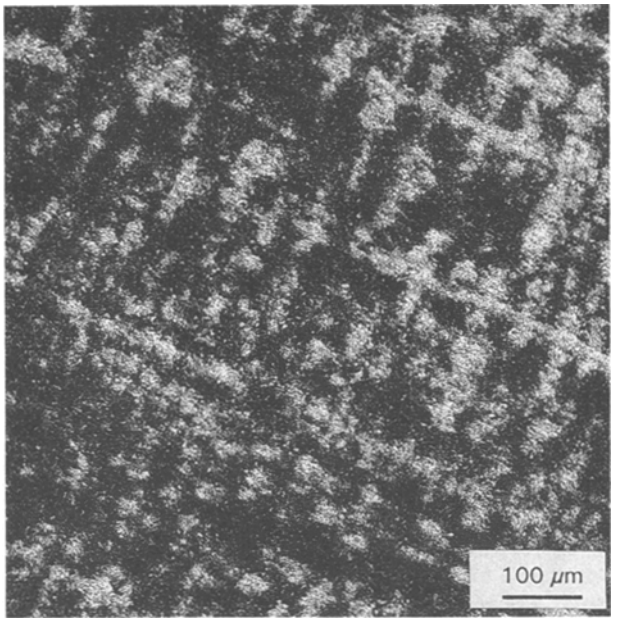

Figure 19 Scanning electron micrograph of the surface of alloy B after coking for 2 h at 1000 °C, showing the morphology of the granular surface carbide reflecting the dendritic structure of the underlying alloy.

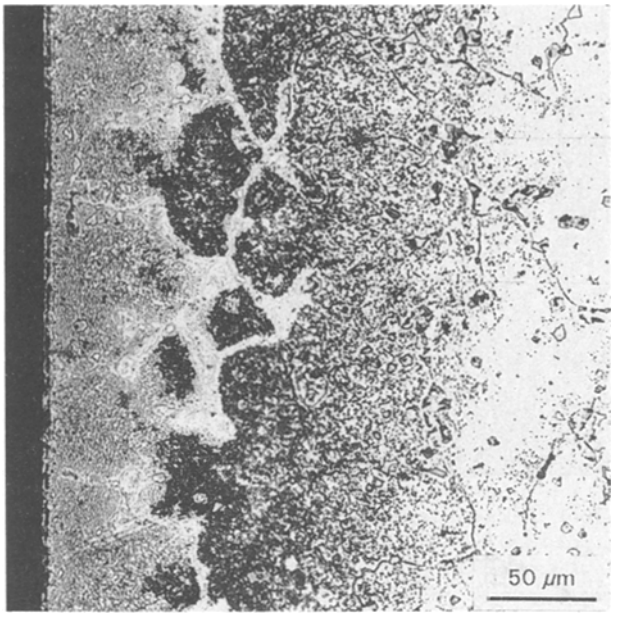

Figure 21 Optical micrograph of a cross-section of alloy G after coking for 2 h at 1000 °C, stained to show extensive internal carburization.

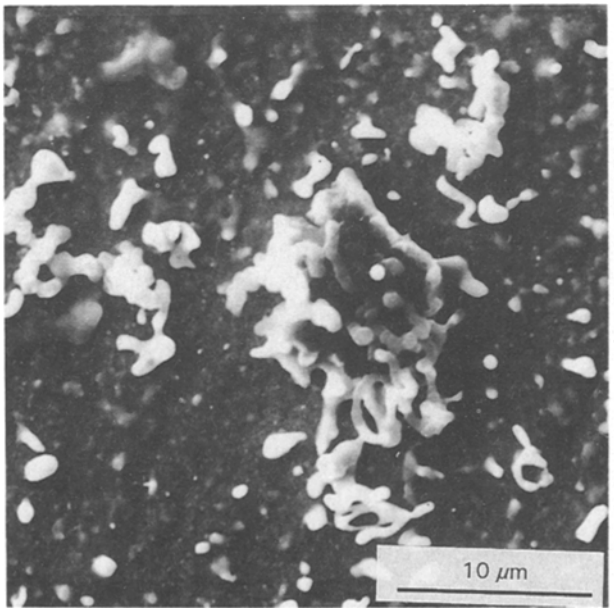

Figure 20 Scanning electron micrograph of the surface of alloy E after coking for 2 h at 1000 °C, showing pyrolytic coke particles on a mixed surface of granular carbide and smooth pyrolytic coke.

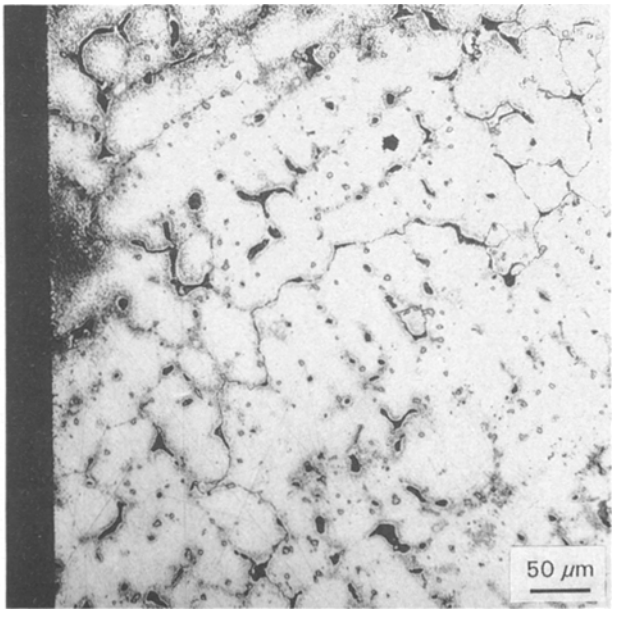

Figure 22 Optical micrograph of a cross-section of alloy H after coking for 2 h at 1000 °C, stained to show only slight internal carburization around dendrite boundaries.

internal carbide formation along dendrite boundaries (Fig. 22). The apparent absence of carbide in the XRD analysis of this alloy, most likely stems from the small volume fraction of carbide formed, in conjunction with the relatively thick covering layer of coke. The surface morphology of this alloy was quite different from that of other alloys. The bulk of the surface was covered in a thick layer of very smooth pyrolytic coke (Fig. 23). In some areas, small clusters of coarse coke filaments grew from this layer, but none had lengths in excess of 10 μm. General surface analysis showed enrichment of chromium, silicon and aluminium. The pyrolytic coke had spalled in places, and the underlying surface contained very little aluminium but an increased chromium level (55 wt % from an original value of 18 wt %), showing that some carbide formation had occurred. Total X-ray yields in EDX analysis of coke-covered areas were a factor of five lower than those from coke-free areas, indicating the coke layer to be much thicker than those observed on the other alloys. The original grinding marks on alloy H were replicated in the coke layer, whereas this was not the case for the other alloys (e.g. Fig. 20). This indicated that during the initial stages of the test at least, the surface of alloy H was not affected by carbide growth.

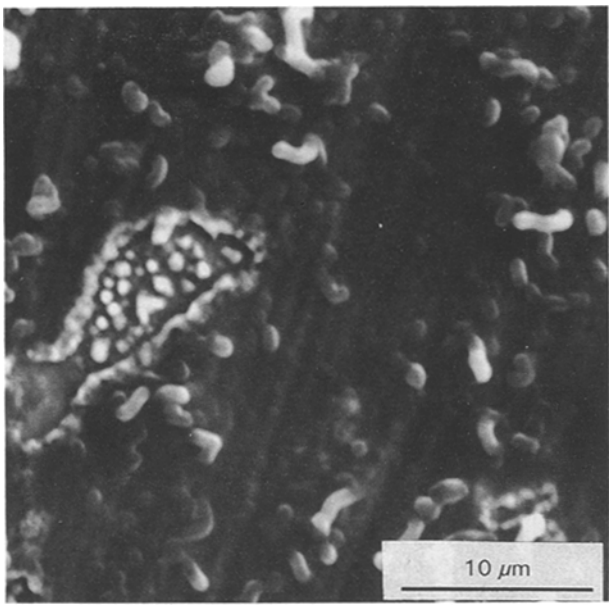

Figure 23 Scanning electron micrograph of the surface of alloy H after coking for 2 h at 1000 °C, showing a smooth and relatively thick layer of pyrolytic coke formed on the surface. The alloy grinding marks are reproduced in the coke layer suggesting little carburization attack.

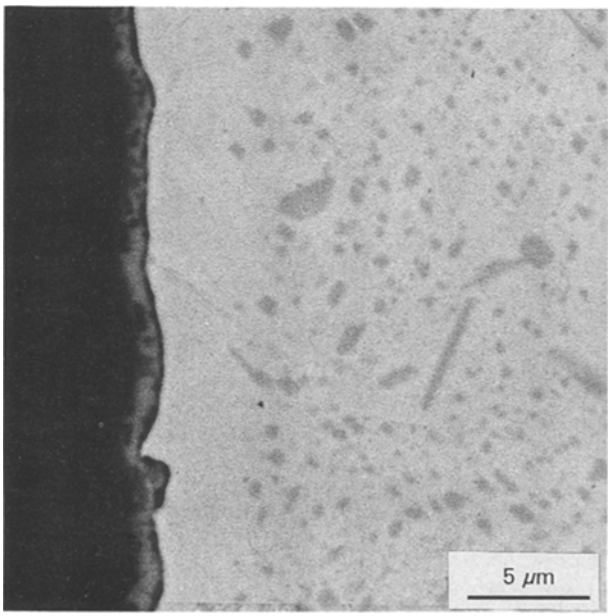

Figure 24 Scanning electron micrograph of a cross-section of alloy A after pre-oxidation in dry air at 900 °C for 200 min, coking at 1000 °C for 1 h, cooling to room temperature, then coking for a further 1 h at 1000 °C. A chromium-rich carbide scale containing oxide particles has formed, resulting in the formation of a carbide-depletion zone in the underlying carburized alloy.

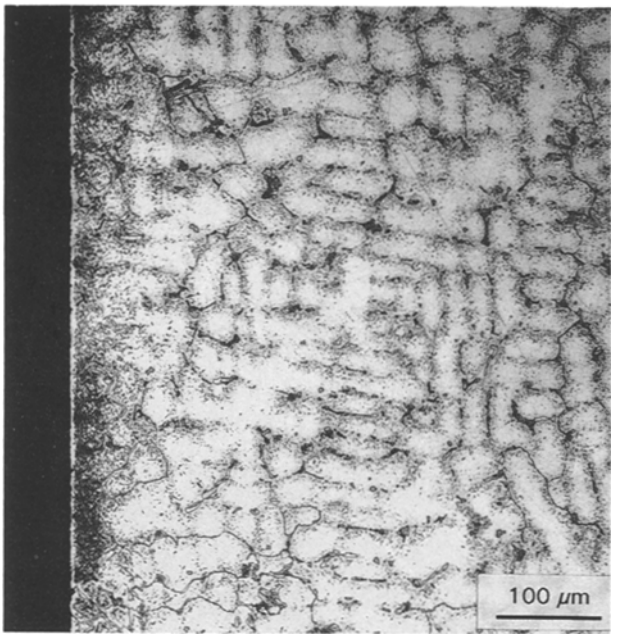

Figure 25 Optical micrograph of a cross-section of the specimen shown in Fig. 24, stained to show the limited internal attack as a result of pre-oxidation.

Alloy A which had been oxidized prior to coking (Fig. 7), formed a thin (≈ 1 μm), adherent external scale (Fig. 24). This scale was comprised of two phases and analysis showed it to be chromium-rich. A carbide-depletion zone beneath the scale was also evident, as was internal carburization. The depth of this carburization zone (Fig. 25) was much lower (by a factor of four) than that of the non-pre-oxidized specimen. In the absence of pre-oxidation, alloy A underwent attack comparable to that of alloy G (Fig. 21). In the optical microscope the two-phase external scale appeared to be comprised of particles of dark oxide in a metallic-looking carbide scale. XRD analysis showed the scale to be predominantly M_7C_3 with $(Fe, Cr)_3O_4$ and coke also present.

4. Discussion

Alloy behaviour can be divided into two temperature ranges. At and below 800 °C the carbon uptake kinetics were mainly linear, while at 900 and 1000 °C

they were predominantly parabolic. Similar studies [20, 21] conducted on a range of cast austenitic alloys showed a similar distinction. This was accompanied by a change in the principal mechanism of coke deposition from the gas stream. At low temperatures, the range of which varied with alloy composition, heterogeneous catalysis of hydrocarbon decomposition occurred. Such catalytic deposits were characterized by coke in the form of filaments, often with nickel-rich particles at their growing tips. Catalytic decomposition kinetics are linear [21], and this would account for the linear kinetics observed at and below 800 °C.

4.1. Low-temperature behaviour (700–800 °C)

The absence of significant internal attack at 700 °C indicates that the relatively large spread in weight-gain rates must result from differing catalytic activities of the surfaces. At 800 °C mild internal attack was found for alloys B, D and E only. Alloy E was the only alloy to exhibit parabolic weight gain kinetics at this temperature, suggesting that the rate of carbon entry into this alloy, as well as the surface deposition rate were important. A similar change from linear kinetics following the onset of internal carburization has been reported by Jackson *et al.* [20].

The scale formed at the two lower temperatures was a relatively heavily fragmented, and poorly adherent carbide, M_7C_3. This scale has been shown to possess little catalytic activity towards the deposition of coke [20, 21, 26], as evidenced here by the localized formation of filamental coke bundles at defect sites. During the early stages of reaction, therefore, it might be anticipated that the rate of deposition would decrease with time, as the available alloy surface area diminished under a developing scale. This was indeed found to be the case for many of the alloys tested here (Figs 1 and 2), where the more rapid weight gains were evident in the early stages. The chromium-rich M_7C_3 scales formed here are not protective in the longer term, however [14], and subsequent cracking or spalling leads to the exposure of a substrate depleted in chromium, and therefore enriched in iron and nickel. The exposed alloy catalyses coke deposition at these localized scale defects [17, 22]. M_3C_2 carbide scales are more protective than M_7C_3 [14], but were not detected on any alloys, except tentatively on alloy F at the highest temperature. The loose correlation between the weight-gain kinetics and the density of surface coke nodules, suggests that it is the variable protectiveness of these surface carbide layers, which contributes to the wide range of kinetic behaviour observed at lower temperatures.

All alloys produced fairly similar deposit morphologies at 800 °C, with the surface being covered by a granular chromium-rich scale, scattered with small nodules of tightly interwoven coke filaments, along with some longer trailing filaments. Very similar morphologies have been observed in a similar study [26]. In the present case, these nodules often appeared to replicate the dendritic structure of the underlying alloy. This was presumably due, in part, to texture effects in the substrate. In addition, the interdendritic regions contained a chromium rich (≈ 60 wt %) $M_{23}C_6$ carbide. External chromium carbide scales formed in the vicinity of such precipitates might be more prone to localized failure due to stresses generated in the scale. These could occur as a result of the different volume changes associated with the conversion of alloy chromium and $M_{23}C_6$ at the surface into M_7C_3, and the different scale thicknesses caused by the different alloy chromium concentrations in the two alloy phases.

A wide range of coke deposition rates was observed at 700 and 800 °C, whereas at higher temperatures a much narrower range of weight gains was displayed by nearly all alloys. At higher temperatures, homogeneous gas-phase pyrolysis occurs, and it has been suggested that the deposition rate of coke on the alloy surface is not influenced by its composition [20]. In contrast, the heterogeneous catalytic process is strongly dependent on surface composition. This was evident in experiments where at and below 800 °C little coke was deposited on the reactor wall (Vycor is non-catalytic towards coke deposition [27]), while at higher temperatures, heavy deposition occurred.

In the present case, there appeared to be a relationship between alloy iron/nickel ratio and the coking rate at 700 °C. The k_{lin} values for the four alloys tested decreased with increasing iron/nickel ratio. At 800 °C this pattern was reversed, with the alloy having the highest iron/nickel ratio also having the highest k_p value (alloy A). The rate of coke deposition was found to decrease with iron/nickel ratio, but the dependence was not strong.

Alloy H, which displayed significantly lower rates than the rest of the alloy set at the two highest temperatures, did not differ drastically from the other alloys at 800 °C. It did, however, gain weight significantly slower than alloys A and D. While other compositional differences were significant, the 5 wt % surface concentration of aluminium in alloy H was probably an important factor. An aluminized 30–23 austenitic steel with a high aluminium surface concentration has been shown to coke at one-sixth the rate of the untreated steel, owing to the low catalytic activity of aluminium-rich surfaces [27].

Catalytic, nickel-rich particles were conclusively observed only on alloy A. TEM studies on such particles have been reported [17, 20–22, 28, 29], and various theories have been proposed to account for their origin [17, 22, 29]. The present study showed that the particles were facetted, with a {1 1 1} facet at the particle head. Audier *et al.* [28] have reported similar findings. Amorphous filaments were observed to grow from higher index planes at the particle sides and rear. The origin of this morphology is probably due to coke deposition on the {1 1 1} facet and subsequent lateral diffusion to growth sites at the particle sides. The rate of coke deposition on nickel has been shown to be fastest on the {1 1 1} plane [22, 30], and the most likely driving force for diffusion is surface-energy differences between the particle head and sides, stemming from the marked facetting, and the small radius of

curvature of the particle [31]. The apparent absence of metallic particles within the growing coke on the other alloys, does not necessarily imply a different growth mechanism for such filaments, because filament growth has been shown to occur readily from particles or active sites attached to an alloy substrate [17].

4.2. High-temperature behaviour (900–1000 °C)

At 900 °C and 1000 °C, the kinetics were found to change from mainly linear to parabolic. This indicated that a process under diffusion control was dictating the weight-gain kinetics. Examination of cross-sections showed that internal carburization attack was extensive at both these temperatures (Table III). The relatively large spread in weight gain kinetics at 800 °C disappeared at and above 900 °C (excluding alloy H), and a change in the surface reaction products was observed. At 900 °C, some filamental coke was still present, though examination in section showed that most of the coke was of a compact pyrolytic type. Alloy H was covered with coke filaments (Fig. 18a), similar to those seen on the other alloys only at lower temperatures.

At 1000 °C filamental coke was entirely absent from all alloys (Figs 19, 20, 23). Alloys A–C were the only ones to form relatively thick external carbide scales, and these alloys exhibited some of the highest k_p values at this temperature (Table II). Similar scales have been observed to form under isothermal carburization testing [16], although they tended to spall and disintegrate after several hours exposure. These alloys did not contain reactive element additions (Table I). Such additions have been shown to confer good carburization resistance in this temperature range [16].

The change from catalytic coke formation at 800 °C to pyrolytic coke formation at 1000 °C would not be expected to alter the nature of the kinetics, because both these processes result in linear kinetics [20]. The parabolic rates observed here, undoubtedly stem from the diffusion-controlled internal carburization process. This is evident from the close correlation between weight-uptake rates and carburization depths shown in Tables II and III. The behaviour of alloy H confirmed this, because this alloy experienced weight-change rates lower by an order of magnitude than any of the other alloys, and also experienced minimal internal attack (Fig. 22). It should be pointed out that under circumstances where alloy H exhibited parabolic kinetics, the carburization kinetics cannot be meaningfully compared with k_p values for the other alloys, because the nature of the internal attack is very different. Rate constants obtained for alloys A–G represent general carburization rates, because internal attack is very uniform on these alloys. However, the value obtained for alloy H represents localized attack at a few locations, while much of the alloy remained unaffected.

The correlation between the weight-gain kinetics and the measured carburization depth can be tested quantitatively by calculating the weight gain caused by internal carbide precipitation. This was done for alloy A assuming the carburization depth to be completely uniform, and that all the elements which could form carbides did so. The initial chromium concentration was modified to take into account primary carbide formation, assuming that all carbon originally in the alloy reacted with chromium exclusively to produce $Cr_{23}C_6$. The effect of differing stoichiometries of the carbides was included. In the case of chromium, it was assumed that the carburized zone consisted of equal thicknesses of Cr_7C_3 and $Cr_{23}C_6$. The effect of external coke and carbide layers was neglected. Based on a depth of 180 μm formed at 1000 °C, alloy A would be expected to have gained 5.5 mg due to carburization. The measured value was in reasonable agreement at 4.5 mg. The k_p values and activation energies obtained here agree well with those of other studies [20].

Alloy H exhibited very low weight gains and limited internal attack when compared to the other alloys at and above 900 °C. However, in longer-term isothermal carburizing and steam-carburizing tests [16, 24], this alloy behaved quite poorly. This apparent discrepancy arises from the much shorter time scales of the tests described here. Analysis has shown [24] that aluminium enrichment is significant on the surface of this alloy, and a very thin protective scale containing Al_2O_3 is thought to form, mainly during the heating up stage [13, 32]. Owing to its very high thermodynamic stability, this oxide can persist even under strongly reducing conditions [32]. However, once this scale fails, internal carburization is rapid due to the low alloy silicon and chromium levels (Table I). The surface of alloy H at 1000 °C was covered with a dense, uniform layer of pyrolytic coke (Fig. 23), identified by XRD as being graphitic. Thick deposits of this type were absent at this temperature from the other alloys, which tended to form surface carbide layers with only limited pyrolytic coke.

It would appear that the protective oxide scale which forms on alloy H slows the ingress of carbon significantly, prevents external carbide formation, and enables the build-up of coke on the surface. Because internal carburization is much faster on the other alloys, carbon dissolution into the alloy, rather than coke build-up at the surface is favoured. This was demonstrated clearly for alloy A at 1000 °C (Fig. 8), where the overall rate-determining process (carburization) was parabolic ($k_p = 22.25 \times 10^{-3}$ mg^2 cm^{-4} min^{-1}), and the rate of coke build-up on the surface, which was much slower, was linear ($k_{lin} = 1.1 \times 10^{-3}$ mg cm^{-2} min^{-1}).

Values have also been obtained for the linear rate constant for coke build-up where carburization is not rate determining, i.e. where carburization has been slowed significantly, or even stopped completely by the presence of an oxide film. The measured rate of weight gain is then the rate of coke deposition on coke. The linear rate obtained for alloy H (Fig. 5) in a test where it displayed linear kinetics was 4.3×10^{-3} mg cm^{-2} min^{-1}. The linear rate for passivated alloy B (Fig. 6) was 4.2×10^{-3} mg cm^{-2} min^{-1}. The rate for pre-oxidized alloy A (Fig. 7) was 4.6

$\times 10^{-3}$ mg cm^{-2} min^{-1}, while the rate for an Fe17Cr 4.5Al alloy, which has been shown to be completely immune to carburization under these conditions [23], was 4.7×10^{-3} mg cm^{-2} min^{-1}. These values show that the rate is effectively constant irrespective of the alloy composition. A similar observation has been made by Holmen *et al.* [19].

Clearly the rate of coke build-up where carburization is occurring rapidly, is much slower (by a factor of four) than the rate of coke build-up in the absence of carburization. Only after about 200 min did the rate of coke build-up on alloy A increase. Because most coking tests were conducted for 120 min at this temperature, the absence of significant amounts of coke on the surfaces of alloys A–G at the highest temperature is therefore explained. Jackson *et al.* [20] have reported an absence of surface coke on HK40 after 4 days coking, as a consequence of the carbon dissolving in the alloy, contributing to internal carburization. Compared to the rate of coke build-up on alloy A (Fig. 8) during the first 200 min ($k_{lin} = 1.1 \times 10^{-3}$ mg cm^{-2} min^{-1}), the subsequent rate was 4.2×10^{-3} mg cm^{-2} min^{-1}. This was much closer to the rate of coke build-up on coke (4.7×10^{-3} mg cm^{-2} min^{-1}). This suggests that once a critical amount of coke has built up, a large proportion of the surface becomes encapsulated. Further coke build-up then proceeds at a rate characteristic of coke deposition on coke.

The changes in weight gain kinetics from parabolic to linear, which occur at this time, are a consequence of coke encapsulation. The encapsulation of sufficient surface sites at which dissolution of carbon from the gas phase is occurring leads to a slowing of the rate of carbon ingress. The rate of carbon diffusion into the alloy is then no longer the rate-determining step. However, dissolution of carbon into the alloy was still occurring after encapsulation, because after about 200 min, the overall rate of weight gain, which had become linear (Fig. 9), was 1.1×10^{-2} mg cm^{-2} min^{-1}. This rate was twice that of coke build up on coke. This indicates that encapsulation was not complete, otherwise the overall rate would be reduced to that of coke deposition on coke. Carbon dissolution could still occur at sites not encapsulated, either directly from the gas phase, or more slowly, by dissolution of the coke deposit.

Following the development of an oxide film on an alloy surface, low rates of weight gain ensue compared to the rates measured when carburization is occurring. This was demonstrated by the passivation and pre-oxidation experiments, which showed that rates of weight gain were reduced by over an order of magnitude due to the presence of an oxide film. Here the rate-determining step was coke build-up on the surface, not carbon dissolution and diffusion into the alloy. The principal mechanism by which carbon dissolves into the alloy, appears to be directly from the gas phase, rather than via a solid coke intermediate formed on the surface. If this were not so, then the maximum rate of weight uptake could never exceed the rate of coke deposition. Dissolution of the surface coke deposit into the alloy does occur, but at a rate much slower than that of direct dissolution of carbon from the gas phase. This explains why the overall rate of weight gain is slowed following encapsulation by coke, because the coke film acts as a barrier between the gas phase and the actively carburizing alloy. The close correlation between the weight gain kinetics and the extent of internal attack, shows that above 900 °C it is the intrinsic carburization resistance of the alloys which is the principal factor controlling the overall weight gain kinetics prior to encapsulation.

Alloy H was the only alloy which did not form significant amounts of carbide. This was because it did not form a thick external scale, nor did it significantly carburize internally. Aluminium enrichment at the surface of this alloy was observed, suggesting the formation of a very thin aluminium-rich scale. It has been postulated that such scales form on aluminium-containing alloys, but an aluminium level of ≥ 2.7 wt % is necessary if scale protectiveness is to be maintained [32].

The formation of oxide films on alloy surfaces was effective in excluding carbon in the short-term. This is because carbon is essentially insoluble in oxides such as Cr_2O_3 [33] and the reduction of oxide to carbide is relatively slow. However, the passivated films formed during specimen heat-up were extremely thin, because they formed under a low oxidizing potential over a short period. They were susceptible to fracture and failure by thermal shock, leading to loss of protection. Growth of coke on and in the scale also facilitates its disruption [2]. The oxide film formed by deliberate pre-oxidation was much thicker and was more resistant to thermal shock. However, within a few hours of subsequent coking, the oxide had been converted to M_7C_3 almost completely. With continued coking, the oxide particles remaining in the scale would have been converted also, because the oxygen partial pressure was clearly too low for chromium oxides to be stable [2, 13, 34]. M_7C_3 scales are not protective against carburization, owing to their tendency to crack and spall [14, 24]. Furthermore, such scales formed from chromium oxide are porous, owing to the 43% volume decrease that accompanies the conversion [13]. The scale formed after coking the pre-oxidized specimens was similar in character to those which formed under mildly oxidizing, carburizing conditions [12, 16]. The presence of oxide within the carbide scale has been shown to improve adhesion, and reduce greatly the flux of carbon through the scale. In the short-term tests performed here, this appeared to be the case, as internal attack was reduced considerably. However, longer exposure leading to conversion of the remaining oxide in the scale, would be expected to cause a loss of this protective effect. It is well known [2, 10, 13] that pre-oxidation is not effective in preventing carbon ingress in longer-term tests, because following conversion of the oxide to M_7C_3, the subsequent carburization rates are essentially the same as for the bare alloy.

5. Conclusion

At and below 800 °C, a wide range of weight-gain kinetics was observed, due to the differing efficacy of

the surface carbide scales in excluding carbonaceous gas from the substrate. This, in turn, was dependent on the alloy composition, though no simple correlation between alloy composition and coking rate could be determined. The coke product was in the form of bundles of fine filaments, which formed at localized defects in the non-catalytic carbide scale. Kinetics were mainly linear, due to the rate of coke build-up on the surface being rate-determining.

The importance of internal carburization on the weight-gain kinetics was evident at and above 900 °C, where the weight-gain kinetics were mainly parabolic. The coke product consisted of filamental and pyrolytic coke at 900 °C while at 1000 °C only pyrolytic coke was formed. There was a similar relative ordering between the degree of internal attack and the k_p values for weight gain. The rate of carbon uptake from the gas stream was an order of magnitude faster for alloys which were actively carburizing, compared with carburization-resistant alloys. This was a consequence of direct dissolution of carbon from the gas phase into the alloy being very rapid, in comparison to solid-state interaction between deposited coke and the alloy.

The rate of coke build-up on the surface of an actively carburizing alloy was slow and linear initially, until complete surface coverage was reached. The rate of coke build-up then increased to a value typical of coke build-up on coke. The onset of this increased rate of coke build-up coincided with a change in the overall weight-gain kinetics from parabolic to linear. This was a consequence of encapsulation of much of the surface by a layer of coke. This protected the alloy from the gas phase, and slowed the overall rate of carbon uptake.

Oxide films formed by either pre-oxidation or heating to temperature (passivation films), were protective in the short term, and resulted in slow linear, rather than fast parabolic kinetics. Oxide scales enriched in aluminium were the most protective. The influence of these oxide scales was due to them blocking carbon ingress into the alloy. Alloys protected by oxide scales all exhibited similar rates of weight-gain, characteristic of coke deposition on coke. Such films offered only short-term protection against carburization, because they were subject to fracture by thermal shock, disruption by coke growth and were readily converted to carbide at low oxygen potentials.

Acknowledgement

This work was supported by the State of North-Rhine-Westphalia, Germany, Department MWMT (Grant TPMW-48-18.1), through Schmidt and Clemens GmbH, Germany.

References

1. G. L. SWALES, in "The behaviour of High Temperature Alloys in Agressive Environments". Book 266/EUR 6814 (The Metals Society, London, 1980) p. 45.
2. H. J. GRABKE and I. WOLF, *Mater. Sci. Eng.* **87** (1987) 23.
3. A. SCHNAAS and H. J. GRABKE, *Oxid. Metals.* **12** (1978) 387.
4. T. A. RAMANARAYANAN and R. PETKOVIC-LUTON, *Corrosion* **37** (1981) 712.
5. H. LEWIS, *Br. Corros. J.* **3** (1968) 166.
6. J. K. STANLEY, in "High Temperature Gas-Metal Reactions in Mixed Environments", edited by J. A. Jansen and Z. A. Foroulis (Metals Society of AIME, New York, 1973) p. 143.
7. R. A. PERKINS, in "Proceedings of the International Conference on the Behaviour of High Temperature Alloys in Agressive Environments", Petten, Netherlands, October 1979.
8. R. H. KANE, *Corrosion* **37** (1981) 187.
9. J. F. NORTON, L. BLIDGEN, S. CANETOLI and P. D. FRAMPTON, *Werkstoffe Korros.* **32** (1981) 467.
10. G. H. MEIR, W. C. COONS and R. A. PERKINS, *Oxid. Metals* **17** (1982) 235.
11. G. M. SMITH, D. J. YOUNG and D. L. TRIMM, *ibid.* **18** (1982) 229.
12. P. THOMAS, D. J. YOUNG and D. L. TRIMM, in "Proceedings of the 9th International Congress on Metallic Corrosion", Vol. **1** (1984) p. 58.
13. P. J. SMITH, O. VAN DER BIEST and J. CORISH, *Oxid. Metals* **24** (1985) 47.
14. S. P. KINNIARD, D. J. YOUNG and D. L. TRIMM, *ibid.* **26** (1986) 417.
15. R. PETKOVIC-LUTON and T. A. RAMANARAYANAN, *ibid.* **34** (1990) 381.
16. D. R. G. MITCHELL and D. J. YOUNG, "Corrosion Asia Conference", NACE, Singapore, September 1992, paper 189.
17. R. T. K BAKER, D. J. C. YATES and J. A. DUMESIC, in "Coke Formation on Metal Surfaces", edited by L. F. Albright and R. T. K. Baker (American Chemical Society, Washington, D.C., 1982) p. 1.
18. D. E. BROWN, J. T. K. CLARK, A. I. FOSTER, J. J. McCARROLL and M. L. SIMS, *ibid.* p. 23.
19. A. HOLMEN, O. A. LINDVAAG and D. L. TRIMM, *ibid.* p. 45.
20. P. R. S. JACKSON, D. L. TRIMM and D. J. YOUNG, *J. Mater. Sci.* **21** (1986) 3125.
21. *Idem, ibid.* **21** (1986) 4376.
22. D. L. TRIMM, *Catal. Rev. Sci. Eng.* **16** (1977) 155.
23. D. R. G. MITCHELL, D. J. YOUNG and W. KLEEMAN, in "Corrosion '92", NACE Annual Conference, Tennessee (NACE, 1992) p. 302.
24. D. R. G. MITCHELL and D. J. YOUNG, unpublished work.
25. D. R. G. MITCHELL, D. J. YOUNG and W. KLEEMAN, in "Proceedings of the 12th International Corrosion Congress", Vol. 4 (NACE, 1993) p. 2625.
26. P. TOMASZEWICZ, P. R. S. JACKSON, D. L. TRIMM and D. J. YOUNG, *J. Mater. Sci.* **20** (1985) 4035.
27. J. C. MAREK and L. F. ALBRIGHT, in "Coke Formation on Metal Surfaces", edited by L. F. Albright and R. T. K. Baker (American Chemical Society, Washington, D.C., 1982) p. 123.
28. M. AUDIER, A. OBERLIN and M. COULON, *J. Crystal Growth* **55** (1981) 549.
29. A. M. BROWN and M. P. HILL, in "Coke Formation on Metal Surfaces", edited by L. F. Albright and R. T. K. Baker (American Chemical Society, Washington, D.C., 1982).
30. A. I. LACAVA, E. D. FERNANDEZ-RAONE, L. L. ISAACS and M. CARABALLO, *ibid.* p. 89.
31. R. E. SMALLMAN, in "Modern Physical Metallurgy", 3rd Edn (Butterworth, London 1976) p. 357.
32. S. ANDO, Y. NAKAYAMA and H. KIMURA, *ISIJ Int.* **29** (1989) 511.
33. I. WOLFE and H. J. GRABKE, *Solid State Commun.* **54** (1985) 5.
34. W. F. CHU and A. RAHMEL, *Oxid. Metals* **15** (1981) 331.

Received 1 October 1992
and accepted 16 February 1994